Journal of Photochemistry & Photobiology A: Chemistry 386 (2020) 112097

Contents lists available at ScienceDirect

Journal of Photochemistry & Photobiology A: Chemistry

journal homepage: www.elsevier.com/locate/jphotochem

# Flavonol dyes with different substituents in photopolymerization

Jian You[a], Hongyuan Fu[a], Di Zhao[a], Tianyu Hu[a], Jun Nie[a], Tao Wang[a,b,*]

[a] Department of Organic Chemistry, College of Chemistry, Beijing University of Chemical Technology, Beijing, 100029, PR China
[b] State Key Laboratory of Optoelectronic Materials and Technologies, Sun Yatsen University, Guangzhou, PR China

ARTICLE INFO

*Keywords:*
Photopolymerization
Photochemistry
Flavonol dyes

ABSTRACT

To further expand the applications of flavonol dyes **(3HFs)** in photopolymerization, six flavonol dyes with different substituents were prepared by using the Algar–Flynn–Oyamada method. The steady-state photolysis and fluorescence quenching of **3HFs** under the 385 nm **LED** light source showed that the proton transfer reaction preceded the charge transfer reaction between **3HFs** and triethanolamine **(TEOA)** or iodonium salts **(ONI)**, and groups with different electron properties could affect the photochemistry of **3HFs**. The influence of substituents on the free radical polymerization efficiencies of **3HFs/TEOA** and **3HFs/ONI** was evaluated. Results showed that charge transfer occurred in the oxidation or reduction processes between **3HFs** and **TEOA** or **ONI**. The possible mechanism was speculated, and the thermal feasibility of charge transfer between **3HFs** and **TEOA** or **ONI** was calculated on the basis of the free energy changes of photoinduced electron transfer.

## 1. Introduction

Flavonol dyes **(3HFs)** have been extensively studied in food and health sciences for their low toxicity and antioxidant and anticancer activities [1–9]. **3HFs** also exhibit excellent optical properties because they are typical molecules of excited state intramolecular proton transfer **(ESIPT)** properties [10–16] (Scheme 1). The **ESIPT** properties of **3HFs** enable them to have large Stokes shifts, dual emission, and reasonable fluorescence quantum yield, which have been used in microbial fluorescence cell imaging studies [17–21]. In 2017, Ushakou et al. demonstrated that 3-hydroxyflavone **(3HF)** was effective for the on-line monitoring of the photopolymerization process in polymer E-Shell 300 with good fluorescence properties [22].

In recent years, using natural products as photosensitizers is important in the photopolymerization technique. For example, curcumin and its derivatives exhibit excellent performance in both free radical polymerization **(FRP)** and cationic polymerization [23,24]. **3HFs** have attracted considerable attention because they are natural products and exhibit photoactivity. Jacques Lalevée et al. synthesized and evaluated some **3HFs** linked to a conjugated system, such as arene, pyrene, or anthracene, as photo-initiator **(PI)** to achieve a high photosensitivity under visible light [25]. They reported that **3HF** could be used as a versatile high-performance visible light **PI** in combination with an amino acid (N-phenylglycine) for the **FRP** of methacrylates in thick samples or composites [26]. Moreover, **3HF** can be used in three-component systems with an iodonium salt (**ONI**) and an amine for the cationic polymerization of epoxides upon exposure to near-UV light **LED**. However, only a few **3HF** with different structures were investigated in the photopolymerization.

Considering **3HFs** will have important application in the photopolymerization technique, we prepared a series of **3HFs** with different substituents and discussed the effect of different substituents on the charge transfer reaction between **3HFs** and amine or iodonium salts. The effect of substituents of **3HFs** on their spectral properties and photoreactivity were also investigated. The structure and abbreviation of **3HFs** with different substituents on rings **A** and **B** are shown in Fig. 1. In the abbreviation of **3HFs**, the letter **A** represents the substituents on ring **A**, while **B** represents the substituents on ring **B**. This study will further expand the applications of **3HFs** in the photopolymerization techique.

## 2. Experimental section

### 2.1. Materials and characterization

All reagents and solvents used were of reagent grade, which were obtained from commercial sources and used without further purification. N-Methylpyrrolidone (**NMP**), 2-hydroxyacetophenone, benzaldehyde, 4-methylbenzaldehyde, 4-fluorobenzaldehyde, 4-chlorobenzaldehyde, 4-bromobenzaldehyde, 2-hydroxy-5-fluoroacetophenoe, and 2-hydroxy-5-bromoacetophenone were purchased from Tianjin Seans Technology Company (Tianjin,China). Triethanolamine (**TEOA**), triethylamine (**TEA**)

* Corresponding author at: Department of Organic Chemistry, College of Chemistry, Beijing University of Chemical Technology, Beijing, 100029, PR China.
*E-mail address:* wangtwj2000@163.com (T. Wang).

https://doi.org/10.1016/j.jphotochem.2019.112097
Received 8 June 2019; Received in revised form 12 September 2019; Accepted 18 September 2019
Available online 20 September 2019
1010-6030/ 

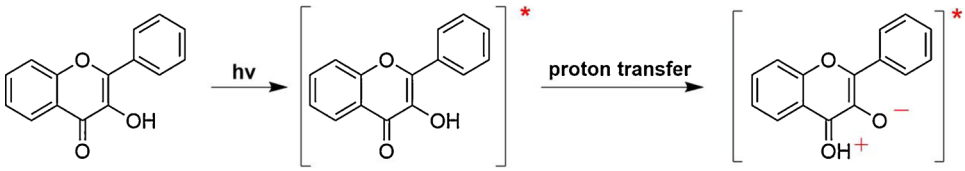


**Scheme 1. ESIPT** property of **3HF-H**.

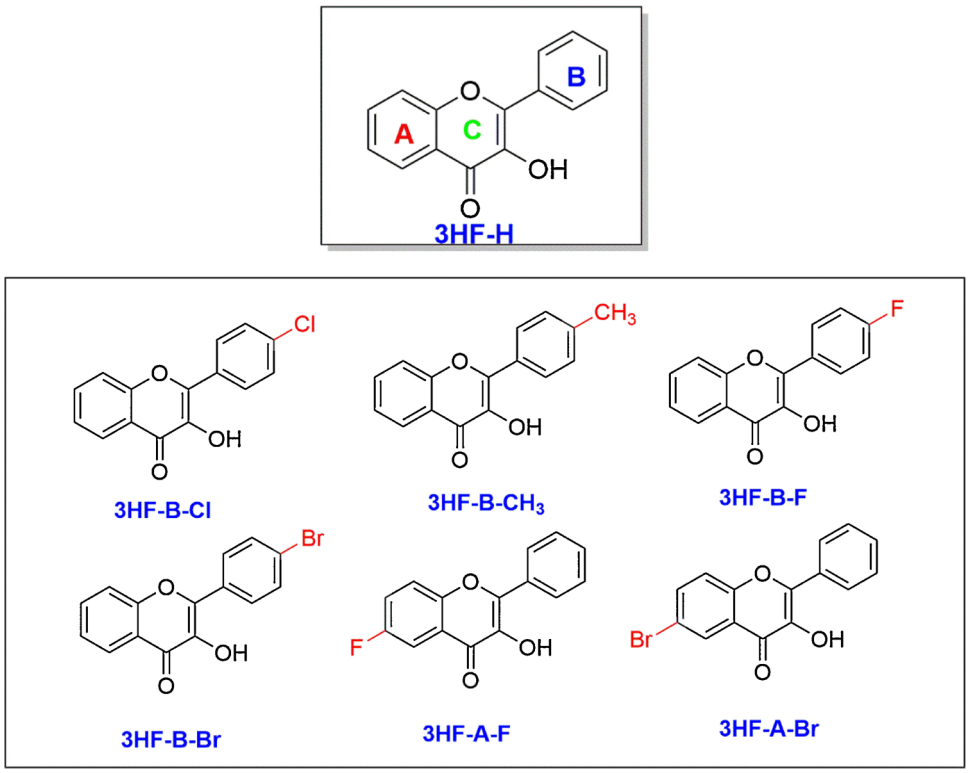


**Fig. 1.** Stucture and abbreviation of **3HFs** with different substituents.

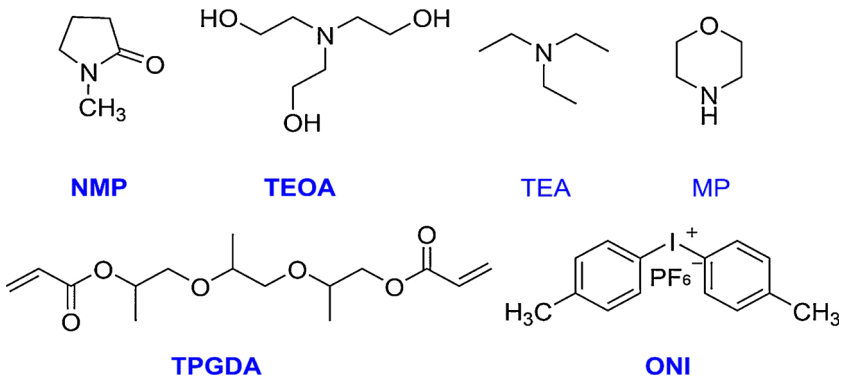


**Fig. 2.** Abbreviations and structures of the compounds used in this study.

and morpholine (**MP**) were purchased from Beijing Chemical Works (Beijing, China). Iodonium bis (4-methylphenyl) hexafluorophosphate was used as a reference iodonium salt (**ONI**). Tripropylene glycol diacrylate (**TPGDA**, from Guangzhou Lihou Trading Co. Ltd, China) was chosen as the monomer for free radical photopolymerization. The abbreviations and structures of the compounds used in this study are listed in Fig. 2.

$^{1}$H NMR (400 MHz) and $^{13}$C NMR (101 MHz) spectra were recorded on a Bruker AV400 NMR spectrometer. IR spectra were recorded on a Nicolet 5700 instrument (Thermo Electron Corporation, Waltham, MA). Melting points were determined on an XT-4 microscopy melting point apparatus. The 385 nm LED light sources were used for the irradiation of the photocurable samples. $I_0 \approx 64$ mW cm$^{-2}$ (3 cm). The UV–Vis spectra were recorded using a UV-5200 (UNICO) UV–vis spectrophotometer. Fluorescence spectra and fluorescence quantum yield were investigated using a FS5 (EDINBURGH INSTRUMENTS) fluorescence spectrometer. LC–MS spectra were recorded on a Agilent HPLC-6500 Series Q-TOF chromatograph.

### 2.2. Synthesis of *3HF* dyes

Process of the preparation of **3HFs** is shown in Scheme 2. The **3-HFs** were synthesized by the method of Algar-Flynn-Oyamada (**AFO**) [27]. Sodium hydroxide (2.0 g, 0.050 mol) was added to a 100 ml round bottom flask, dissolved in 5.0 ml of water, the temperature was lowered

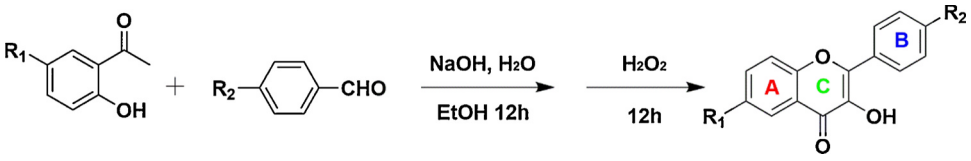


**Scheme 2.** Process of the preparation of **3HFs**.

to room temperature, and then 30 ml of ethanol was added; Next, weigh 6.0 mmol of 2-hydroxyacetophenone or substituted 2-hydroxyacetophenone and 6.0 mmol of benzaldehyde or substituted benzaldehyde were added, and diluted with 20.0 ml of ethanol. After 12 h of reaction, 30% Hydrogen peroxide **($H_2O_2$)** (2.0 ml) was added directly, and the reaction was continued for 12 h. The reaction solution was neutralized with concentrated hydrochloric acid to neutrality. Water was then added to dissolve the inorganic salts produced by the neutralization. At that time, a large amount of solid precipitated. The solid was filtered, and then recrystallized from ethanol.

*2.2.1. 3-Hydroxy-2-phenyl-4H-chromen-4-one (**3HF**)*

$^1$H NMR (400 MHz, DMSO-$d_6$) $\delta$: 8.47 – 7.95 (m, 3 H), 7.96 – 7.22 (m, 6 H); $^{13}$C NMR (101 MHz, DMSO-$d_6$) $\delta$ 172.97, 154.56, 145.15, 139.05, 133.71, 131.27, 129.85, 128.49, 127.63, 124.77, 124.54, 121.28, 118.39; IR (KBr, ($cm^{-1}$)): 3210, 1130 (C—O—H), 1608 (C═O), 1562 (C═C); Yield: 70%; Mp:178–179 °C (170 °C) [28];

*2.2.2. 3-Hydroxy-2-(p-tolyl)-4H-chromen-4-one (**3HF-B-$CH_3$**)*

$^1$H NMR (400 MHz, DMSO-$d_6$) $\delta$ : 8.16 (d, $J$ = 8.1 Hz, 2 H), 8.12 (dd, $J$ = 8.0, 1.6 Hz, 1 H), 7.85 – 7.72 (m, 2 H), 7.47 (ddd, $J$ = 8.0, 6.6, 1.5 Hz, 1 H), 7.38 (d, $J$ = 8.1 Hz, 2 H), 2.40 (s, 3 H); $^{13}$C NMR (101 MHz, DMSO-$d_6$) $\delta$ : 173.10, 154.45, 145.31, 139.61, 139.22, 133.51, 129.08, 128.61, 127.47, 124.72, 124.41, 121.24, 118.34, 21.01. IR (KBr, ($cm^{-1}$)): 3282, 1110 (C—O—H), 1608 (C═O), 1563 (C═C); Yield: 75%; Mp: 197–199 °C (206 °C) [28];

*2.2.3. 2-(4-Fluorophenyl)-3-hydroxy-4H-chromen-4-one (**3HF-B-F**)*

$^1$H NMR (400 MHz, DMSO-$d_6$) $\delta$: 8.30 (dd, $J$ = 8.7, 5.6 Hz, 2 H), 8.13 (d, $J$ = 8.0 Hz, 1 H), 7.80 (dt, $J$ = 16.3, 8.3 Hz, 2 H), 7.46 (dt, $J$ = 16.4, 8.1 Hz, 3 H); $^{13}$C NMR (101 MHz, DMSO-$d_6$) $\delta$: 172.94, 163.83, 161.36, 154.49, 144.37, 138.83, 133.72, 130.06, 127.83, 124.76, 124.56, 121.29, 118.38, 115.70, 115.48; IR (KBr, ($cm^{-1}$)): 3299, 1126 (C—O—H), 1637 (C═O), 1620 (C═C); Yield: 61%; Mp: 147–149 °C (152–154 °C) [29];

*2.2.4. 2-(4-Chlorophenyl)-3-hydroxy-4H-chromen-4-one (**3HF-B -Cl**)*

$^1$H NMR (400 MHz, DMSO-$d_6$) $\delta$: 8.26 (d, $J$ = 8.3 Hz, 2 H), 8.13 (d, $J$ = 7.9 Hz, 1 H), 7.80 (dt, $J$ = 7.4, 8.3 Hz, 2 H), 7.65 (d, $J$ = 8.3 Hz, 2 H), 7.48 (t, $J$ = 7.4 Hz, 1 H); $^{13}$C NMR (101 MHz, DMSO-$d_6$) $\delta$ : 172.97, 154.49, 143.93, 139.30, 134.39, 133.82, 130.16, 129.28, 128.62, 124.78, 124.59, 121.26, 118.39; IR (KBr, ($cm^{-1}$)): 3271, 1127 (C—O—H), 1608 (C═O), 1570 (C═C); Yield: 64%; Mp:186–187 °C (192 °C) [28];

*2.2.5. 2-(4-Bromophenyl)-3-hydroxy-4H-chromen-4-one (**3HF-B -Br**)*

$^1$H NMR (400 MHz, DMSO-$d_6$) $\delta$ : 8.23 – 8.15 (m, 2 H), 8.12 (dd, $J$ = 8.0, 1.6 Hz, 1 H), 7.87 – 7.72 (m, 4 H), 7.53 – 7.44 (m, 1 H); $^{13}$C NMR (101 MHz, DMSO-$d_6$) $\delta$ : 172.97, 154.49, 143.98, 139.35, 133.83, 131.55, 130.51, 129.46, 124.78, 124.60, 123.27, 121.26, 118.39; IR (KBr, ($cm^{-1}$)): 3265, 1125 (C—O—H), 1610 (C═O), 1586 (C═C); Yield: 62%; Mp: 186–188 °C (163–167 °C) [30];

*2.2.6. 6-Fluoro-3-hydroxy-2-phenyl-4H-chromen-4-one (**3HF-A-F**)*

$^1$H NMR (400 MHz, DMSO-$d_6$) $\delta$ 8.23 (d, $J$ = 7.6 Hz, 2 H), 7.89 (dd, $J$ = 9.3, 4.2 Hz, 1 H), 7.78 (dd, $J$ = 8.5, 3.1 Hz, 1 H), 7.72 (td, $J$ = 8.7, 3.1 Hz, 1 H), 7.56 (m, 3 H); $^{13}$C NMR (101 MHz, DMSO-$d_6$) $\delta$: 172.45, 159.60, 157.18, 151.07, 145.63, 138.91, 131.12, 129.97, 128.49, 127.68, 122.29, 122.16, 121.90, 121.28, 109.04; IR (KBr, ($cm^{-1}$)): 3266, 1126 (C—O—H), 1611 (C═O), 1570 (C═C); Yield: 55%. Mp: 159–160 °C (160–161 °C) [31];

*2.2.7. 6-Bromo-3-hydroxy-2-phenyl-4H-chromen-4-one (**3HF-A-Br**)*

$^1$H NMR (400 MHz, DMSO-$d_6$) $\delta$: 8.29 (d, $J$ = 7.7 Hz, 2 H), 8.18 (d, $J$ = 2.4 Hz, 1 H), 7.93 (dd, $J$ = 9.0, 2.5 Hz, 1 H), 7.77 (d, $J$ = 9.0 Hz, 1 H), 7.52 (m, 3 H); $^{13}$C NMR (101 MHz, DMSO-$d_6$) $\delta$: 172.76, 153.30, 145.44, 140.93, 135.91, 131.43, 129.64, 128.42, 127.42, 126.65, 122.75, 121.12, 116.59; IR (KBr, ($cm^{-1}$)): 3289, 1115 (C—O—H), 1600 (C═O), 1554 (C═C); Yield: 58%; Mp: 182–183 °C (180–181 °C) [31].

*2.3. Free radical polymerization (FRP) [24]*

The two-component photoinitiating systems (PISs) are mainly based on **3HFs/TEOA** (1.0%/3.0% w/w) and **3HFs/ONI** (0.20%/1.0% w/w) or (1.0%/0.20% w/w) for the free radical polymerization of methacrylates. The weight percent of the photoinitiating system is relative to the monomer content. The free radical photopolymerization experiments were carried out under laminated conditions. The photosensitive formulations were photocured in 0.6 mm thick plastic molds (Black opaque and does not absorb 385 nm **LED** light) with a 5 mm diameter center. The molds were clamped between two glass slides. The distance between irradiation sources and formulations was 3 cm ($I_0 \approx 64$ mW $cm^{-2}$). The specimens were irradiated at different time intervals by manually controlling the curing light.

The near-infrared spectra of uncured resin were collected by using a Fourier transform near-infrared spectrometer (Nicolet 5700, 4000–7000 $cm^{-1}$ wavelength range); the spectra were obtained immediately after each exposure interval. For each sample, the RT-NIR runs were repeated three times. The double bond conversion profiles were calculated from the decay of the absorption intensities located at 6165 $cm^{-1}$ as described by Stansbury and Dickens [32]. The double bond conversion was calculated using the following equation (Eq. (1)):

$$Conversion\% = |1 - \frac{S_t}{S_0}| \times 100\% \quad (1)$$

where $S_t$ is the area of the C = C characteristic absorbance peak and $S_0$ is the initial area of the C = C characteristic absorbance peak.

*2.4. Steady state photolysis experiments*

In this study, the UV–vis absorption spectrum was used to characterize the photolysis rate of **3HFs** with the change of illumination time. The experimental process is as follows :

The [**3HFs**] = $5.0 \times 10^{-5}$ M solution is prepared.

The samples were irradiated for 0 s, 30 s, 60 s, 120 s, 180 s, 240 s, 300 s, the UV–vis absorption spectra were measured. The distance between the 385 nm **LED** light source and cuvette was 3 cm. The absorbance at 345 nm of the same sample taken at different times was recorded as $A_t$. The photolysis progress was followed by plotting $A_t/A_0$ as a function of irradiation time, where $A_0$ was the initial absorbance of **3HFs** at 345 nm.

*2.5. Fluorescence quenching experiment*

Fluorescence quenching experiments were tested using an FS5 fluorescence spectrometer. The experimental method was similar to the

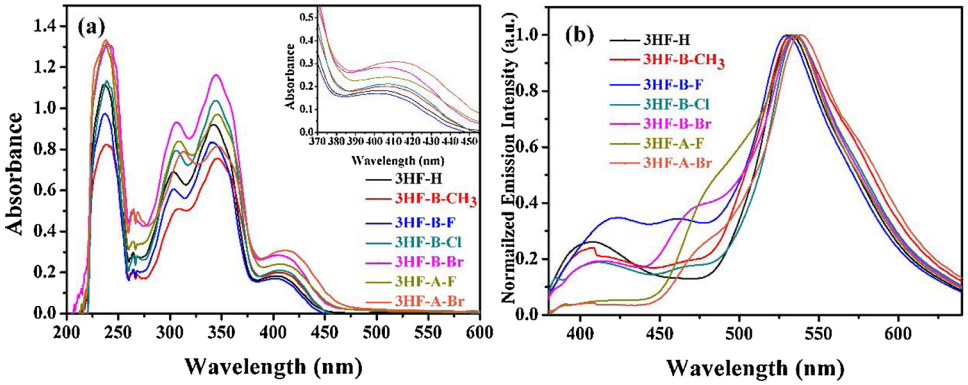


**Fig. 3.** UV–vis absorption spectra (a) and fluorescence spectra (b) of the **3HFs** in methanol (concentration of **3HFs** is $6 \times 10^{-5}$ M).

**Table 1**
Absorption and fluorescence data of **3HFs** in methanol: maximum absorption wavelengths ($\lambda_{max}$), molar extinction coefficients ($\varepsilon$) at $\lambda_{max}$ and at the emission wavelengths of the **LEDs**, maximum emission wavelengths ($\lambda_{em}$), Stokes shift and fluorescence quantum yields ($\Phi_f$).

| 3HF | $\lambda_{max}$ (nm) | $\varepsilon_{max}$ ($M^{-1}*cm^{-1}$) | $\varepsilon_{385}\varepsilon_{385}$ ($M^{-1}*cm^{-1}$) | $\lambda_{em}$ (nm) | Stokes shift($cm^{-1}$) | $\varnothing_f$ (%) |
|---|---|---|---|---|---|---|
| **3HF - H** | 342 | 17789 | 1880 | 532 | 5263 | 5.91 |
| **3HF - B-$CH_3$** | 347 | 14733 | 2607 | 534 | 5347 | 11.20 |
| **3HF - B-F** | 342 | 16225 | 1844 | 529 | 5348 | 5.57 |
| **3HF - B-Cl** | 345 | 19931 | 2120 | 536 | 5263 | 8.39 |
| **3HF - B-Br** | 346 | 20515 | 2237 | 535 | 5291 | 8.09 |
| **3HF - A-F** | 347 | 16879 | 2390 | 534 | 5348 | 9.33 |
| **3HF - A-Br** | 349 | 13815 | 3223 | 539 | 5263 | 11.44 |

photolysis rate test. Fluorescence spectrum was measured at different times for the same sample at the same slit width. The number of photons emitted was represented by the peak area from 360 nm to 670 nm. The number of photons emitted of the same sample taken at different times was recorded as $C_t$. The reaction progress was by plotting $C_t/C_0$ as a function of irradiation time, where $C_0$ was the initial emission intensity.

### 2.6. *3HF-H/TEOA and 3HF-H/ONI interaction*

The solution of **TEOA** (1.00 M) and the solution of **ONI** (1.00 M) were prepared. Then, took 30 μL of **TEOA** solution or **ONI** solution to 3.0 ml of the solution of 3HFs dye($1.0 \times 10^{-4}$ M) and mixed. After the samples were irradiated for 0 s, 30 s, 60 s, 120 s, 180 s, 240 s, 300 s, the UV–vis absorption spectra were measured. Then, took 0 μL, 20 μL, 40 μL, 60 μL, 80 μL, 100 μL, 120 μL, 140 μL, 160 μL, 180 μL, 200 μL, 240 μL of **TEOA** solution or **ONI** solution to 3.0 ml of the solution of **3HF-H** dye ($1.0 \times 10^{-4}$ M) and mixed. So the solutions of **3HF-H** dye with different concentrations of **TEOA** or **ONI** were obtained. Fluorescence spectrum was measured for the same sample at the same slit width and voltage.

### 2.7. *Redox potentials [24]*

Oxidation and reduction potentials in methanol ($CH_3OH$) were measured by cyclic voltammetry (CV) using a CHI760E electrochemical workstation and tetrabutylammonium hexafluorophosphate (0.1 M) as a supporting electrolyte. The concentrations of the 3HFs were $1 \times 10^{-3}$ M. Glassy carbon, Ag/AgCl electrode and a platinum wire were used as the working, reference, and auxiliary electrode, respectively. The ferrocenium/ferrocene ($Fc^+$/Fc) couple was used as the internal standard [33,34]. The glassy carbon electrode was polished with an alumina slurry of 0.3 μm on a polish cloth before use. The platinum wire was immersed in $HNO_3$ solution for 30 min at 80 °C to remove metal impurities prior to use. All the solutions were purged with $N_2$ gas for 10 min before measuring and an $N_2$ gas blanket was maintained over the solution during the experiments. The measured electrode potentials are all converted to electrode potentials with reference to the saturated calomel electrode. The free energy change $\Delta G_S$ for the electron transfer between the excited **3HFs** and **TEOA/ONI** was calculated from the classical Rehm–Weller equation (Eqs. (2) and (3)): [35]

$$E_{SCE} = E_{(Ag/AgCl)} - E_1 + E_2 \quad (2)$$

$$\Delta G_S = F(E_{ox} - E_{red}) - E_S - C \quad (3)$$

where $E_{SCE}$, $E_{(Ag/AgCl)}$ are electrode potential of a reference electrode with a saturated calomel electrode and Ag/AgCl electrode, $E_1$, $E_2$ are ferrocene electrode potential of a reference electrode with a Ag/AgCl electrode and saturated calomel electrode.

$E_1 = E_{(Fc+/Fc)} = 0.29$ V vs. Ag/AgCl, $E_2 = E_{(Fc+/Fc)} = 0.38$ V vs. SCE

where $E_{ox}$, $E_{red}$, $E_S$, F and C are the oxidation potential of the **3HFs** or **TEOA**, the reduction potential of **ONI** or **3HFs**, the excited singlet state energy of the **3HFs**, faraday constant and the electrostatic interaction energy for the initially formed ion pair. (this latter parameter is considered as negligible in polar solvents), respectively.

## 3. Results and discussion

### 3.1. *Absorption and fluorescence emission of 3HFs*

The UV–vis absorption spectra of the studied **3HFs** in methanol are presented in Fig. 3a, and the main data are listed in Table 1. The absorption peaks of **3HFs** with different substituent groups occurred at approximately the same wavelengths from the UV to visible regions. The absorption peaks attributed to the conjugated system in **3HFs** could be observed at 280–450 nm, which showed different absorption strength with different substituent groups. For example, the order of absorption strength at 345 nm is **3HF-B-Br** > **3HF-B-Cl** > **3HF-A-F** > **3HF-H** > **3HF-B-F** > **3HF-A-Br** > **3HF-B-$CH_3$**, whereas that at 385 nm is **3HF-A-Br** ≈ **3HF-B-Br** > **3HF-A-F** > **3HF-B-Cl** ≈ **3HF-B-$CH_3$** > **3HF-H** ≈ **3HF-B-F**.

The fluorescence spectra of **3HFs** in methanol are presented in Fig. 3b, and the main data are listed in Table 1. The **3HFs** have a double emission peak. The two emission bands that were observed corresponded to the fluorescence from the Franck–Condon excited state (emission at approximately 450 nm) and the tautomer produced by **ESIPT** (emission at approximately 550 nm) [10,14]. The substituent group slightly affected the emission of **3HFs** at 550 nm. However, the emission at approximately 400 nm showed obvious differences for different substituent groups. For example, the emissions of **3HF-A-F** and **3HF-A-Br** at approximately 400 nm disappeared, probably due to the rapid **ESIPT**. The emission property of **3HF-B-$CH_3$** was almost the same

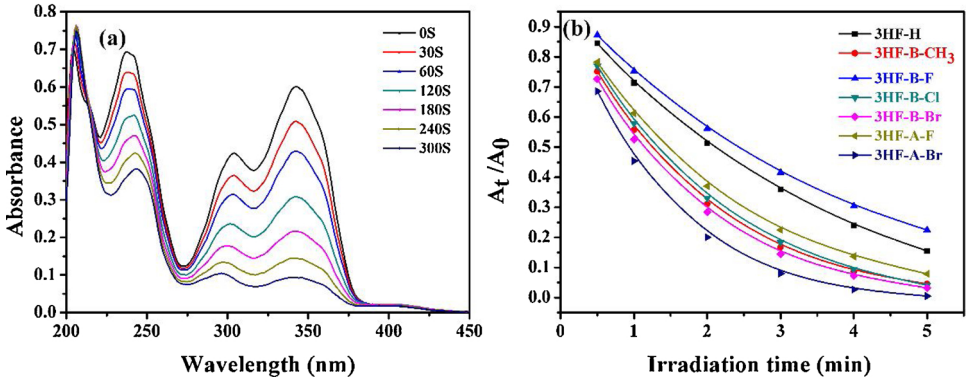


**Fig. 4.** Absorption spectra of **3HF-H** in methanol at different illumination time under the 385 nm **LED** (a); Photolysis rates of different substituted **3HFs** in methanol under the 385 nm **LED** (b). ([3HFs] = $5.0 \times 10^{-5}$ M).

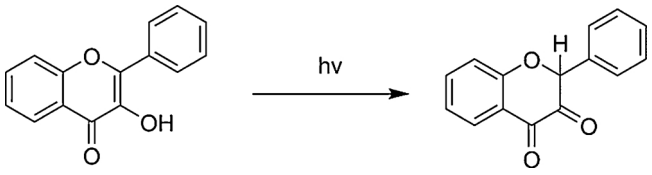


**Scheme 3.** Hydrogen atom transfer process of **3HF-H**.

as that of **3HF-H**.

### 3.2. Steady state photolysis of *3HFs, 3HFs /TEOA and 3HFs /ONI*

Many reports showed that **3HFs** are unstable [36–40]. Under the light conditions, intramolecular proton transfer [10–13,41–46], reverse proton transfer [47], photorearrangement reaction [48,49], photooxidation [50–52], and other reactions can occur. To study the photochemical properties of **3HFs**, photolysis experiments of **3HFs** were carried out under the 385 nm **LED**. The effects of triethanolamine **(TEOA)** and **ONI** on the photolysis of **3HFs** were investigated.

The absorption spectra of **3HFs** with different irradiating times were obtained. As an example, the changes of the absorption of **3HF-H** in methanol with illumination time are shown in Fig. 4a. The changes of the absorption of other **3HFs** in methanol with illumination time are shown in the supplementary part (Figs. S34–S39). As the illumination time increased, the absorbance decreased, but the peak shape remained almost unchanged, which indicates that most of the molecules may undergo photobleaching by hydrogen atom transfer reactions during the illumination (Scheme 3).

According to the change of absorption at 345 nm, the photolysis rates were obtained. Fig. 4b shows that substituents have a large influence on the hydrogen atom transfer in **3HFs**. The photolysis rate sequence is **3HF-A-Br** > **3HF-B-Br** > **3HF-B-CH$_3$** > **3HF-B-Cl** > **3HF-A-F** > **3HF-H** > **3HF-B-F.**

**3HF-H, 3HF-B-CH$_3$** and **3HF-A-Br** were selected as three representative molecules. The photolysis rates of **3HFs /TEOA** and **3HFs /ONI** in methanol were also obtained at the same irradiating condition to study the effect of **TEOA** and **ONI** on the photolysis of **3HFs** (Fig. 5). It can be seen that the addition of **TEOA** to the **3HFs** solution has little effect on the photolysis rates of **3HF-H**, **3HF-B-CH$_3$** and **3HF-A-Br,** but the addition of **ONI** to the **3HFs** solution has large effect on the photolysis rates.

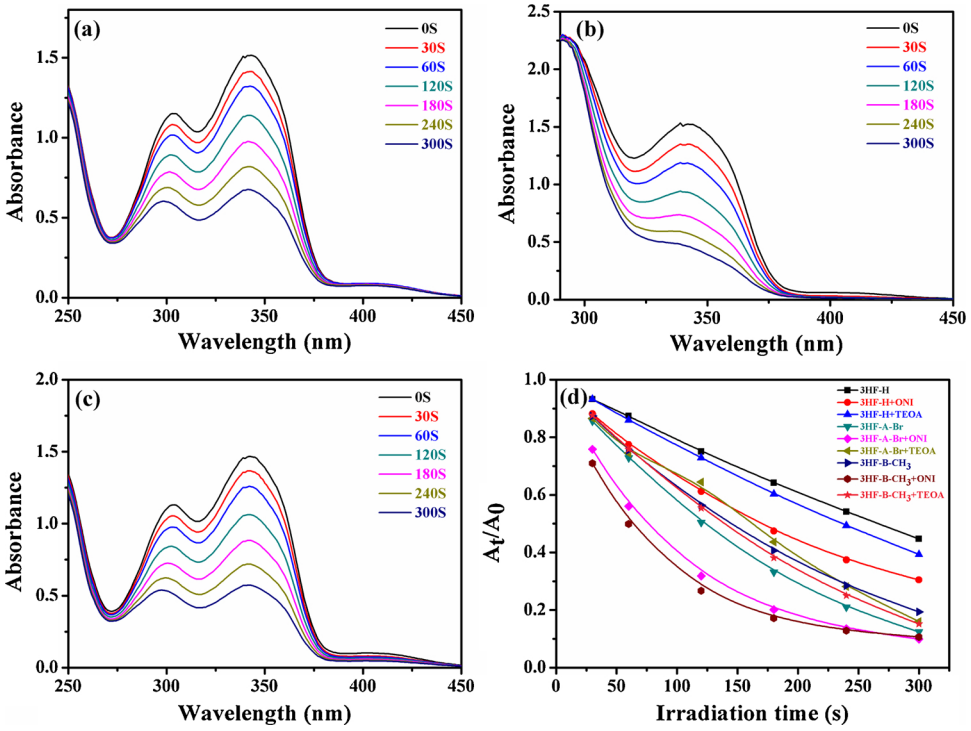


**Fig. 5.** Absorption spectra of **3HF-H** in methanol at different illumination time under the 385 nm **LED** (a); Absorption spectra of **3HF-H/ ONI** in methanol at different illumination time under the 385 nm **LED** (b). Absorption spectra of **3HF-H /TEOA** in methanol at different illumination time under the 385 nm **LED** (c). Photolysis rate of **3HF-H**, **3HF-H/ONI**, **3HF-H/ TEOA**, **3HF-A-Br**, **3HF-A-Br/ONI**, **3HF-A-Br/ TEOA**, **3HF-B-CH$_3$**, **3HF-B-CH$_3$/ONI**, **3HF-B-CH$_3$/TEOA** in methanol under the 385 nm **LED** (d).([3HFs] = $1.0 \times 10^{-4}$ M, [TEOA] = 10 mM, [ONI] = 10 mM).

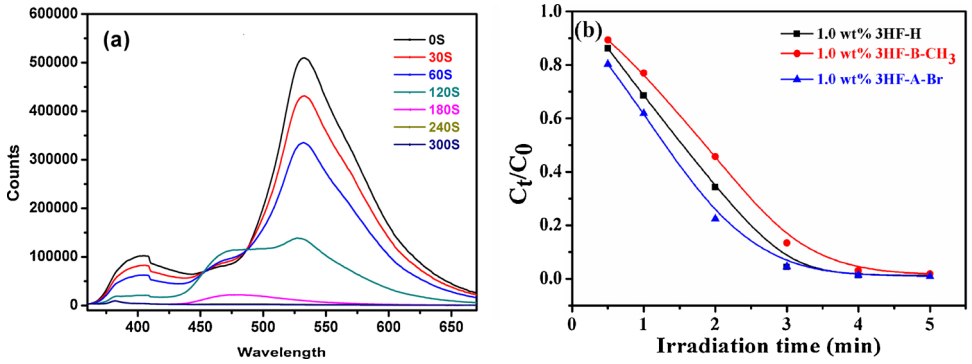


**Fig. 6.** Fluorescence spectra of **3HF-H** in methanol at different illumination time under the 385 nm **LED** (a); fluorescence quenching rate of **3HF**, **3HF-B-$CH_3$**, **3HF-A-Br** in methanol under the 385 nm **LED** (b). ([3HF-H] = $1.68 \times 10^{-4}$ M, [3HF-B-$CH_3$] = $1.59 \times 10^{-4}$ M, [3HF-A-Br] = $1.26 \times 10^{-4}$ M).

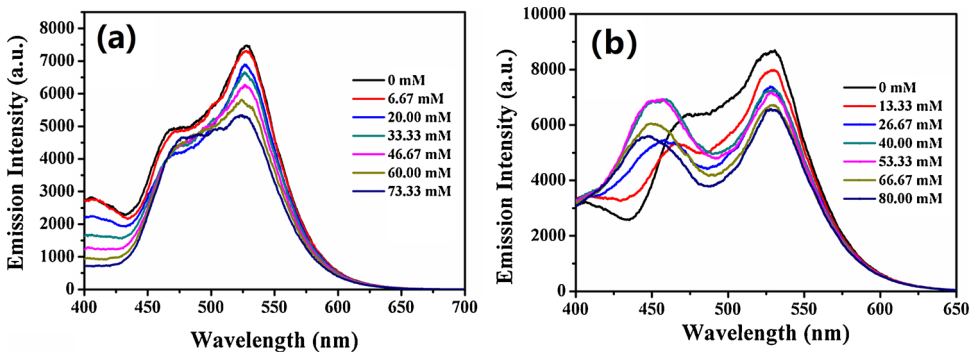


**Fig. 7.** Fluorescence quenching of **3HF-H** by different concentrations of **TEOA** in methanol (a);Fluorescence quenching of **3HF-H** by different concentrations of **ONI** in methanol(b). ([3HF-H] = $1.0 \times 10^{-4}$ M).

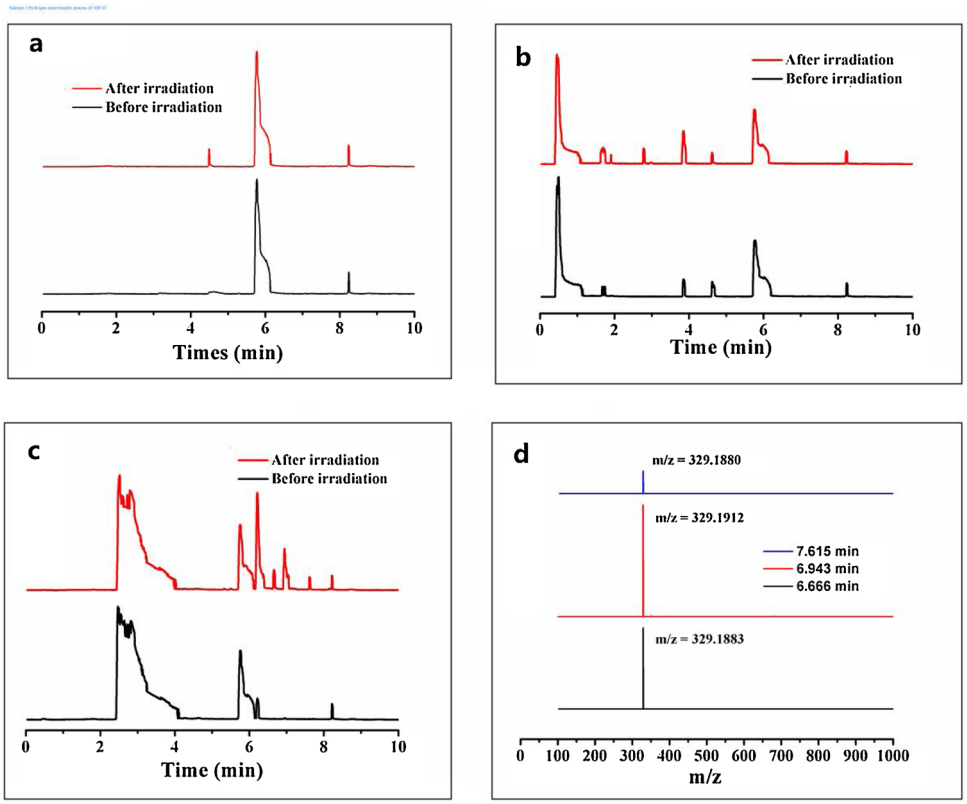


**Fig. 8.** Liquid chromatography of **3HF-H** (a) in methanol before and after 5 min of illumination at 385 nm **LED**; **3HF-H /TEOA** (b) and **3HF-H/ONI** (c) in acetonitrile before and after 5 min of illumination at 385 nm **LED**; The **MS** results of **3HF-H/ONI** in acetonitrile after 5 min of illumination at 385 nm **LED** (d).

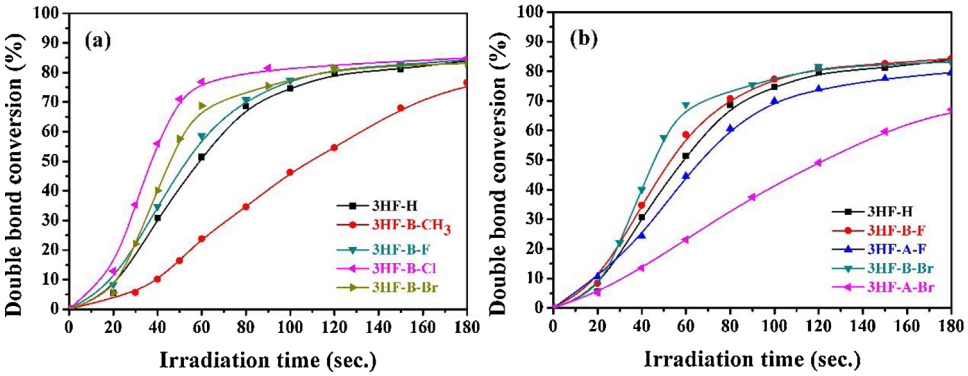


**Fig. 9.** Photopolymerization profiles of **TPGDA** in the presence of **3HFs/TEOA** (1.0%/3.0% w/w) under the 385 nm **LED**.

The fluorescence spectra of **3HF-H**, **3HF-B-CH$_3$**, and **3HF-A-Br** in methanol were studied with illumination time. In Fig. 6a, the emission peak produced by the **3HFs** tautomer is quenched with the illumination time. Fig. 6b shows that substituents have a large influence on the fluorescence quenching of **3HFs** tautomer with the illumination time. These results show that hydrogen atom transfer may occur during photolysis and form a non-fluorescent substance by destroying the conjugated structure of the ring, so the absorbance is reduced and the fluorescence is quenched. Hydrogen atom transfer process of **3HF-H** is shown in Scheme 3.

### 3.3. *3HF-H/TEOA and 3HF-H/ONI interaction*

Fluorescence quenching experiments of **3HF-H** by high concentrations of **TEOA** and **ONI** were carried out and the results were shown in Fig. 7. Fluorescence quenching processes of **3HF-H** by **TEOA**or by **ONI** was noted. The emission of the tautomer produced by **ESIPT** (emission at approximately 550 nm) decreased with the increase of the concentration of **TEOA** or **ONI**.

To investigate the product of photolysis of **3HFs**, **3HFs/TEOA** and **3HFs/ONI** in solution, the LC–MS of these solutions after being irradiated 5 min were obtained. The results of liquid chromatography of **3HF-H** in methanol before and after 5 min of illumination at 385 nm **LED** are shown in the Fig. 8a. The results show that there is only one new product from photolysis of **3HF-H** in methanol and the content of this new product is < 2.0%. The results from the liquid chromatography of **3HF-H/TEOA** in acetonitrile before and after 5 min of illumination at 385 nm **LED** are shown in Fig. 8b. Only two new products with less than 2.0% of content were found. So, it can be concluded that the photolysis of **3HF-H** and **3HF-H/TEOA** is difficult to carry out. The liquid chromatography of **3HF-H/ONI** in acetonitrile before and after 5 min of illumination at 385 nm **LED** is shown in Fig. 8c. It can be seen that three new products were produced. According to the **MS** results (Fig. 8d), one of these products is the isomer of 3HF- toluene derivatives from the reaction of **3HF-H** with toluene free radical from the photolysis of **ONI**. The real structure of 3HF- toluene derivatives can't be characterized.

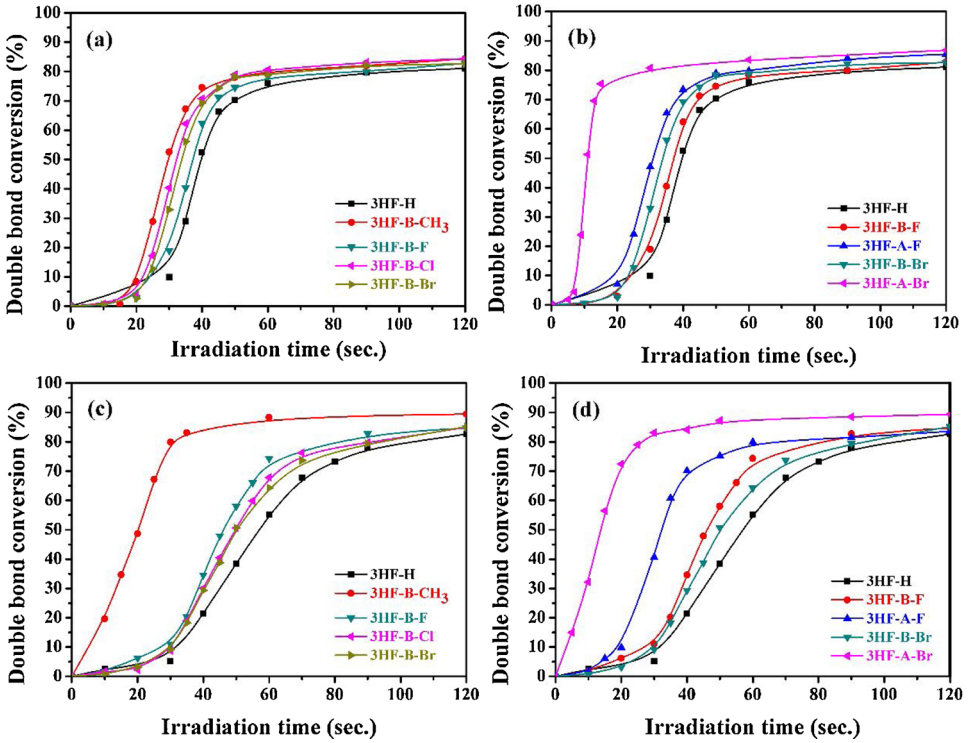


**Fig. 10.** Photopolymerization profiles of **TPGDA** in the presence of **3HFs/ONI** under the 385 nm **LED**. (a) and (b) is **3HFs/ONI** (0.20%/1.0% w/w); (c) and (d) is **3HFs/ONI** (1.0%/0.20% w/w).

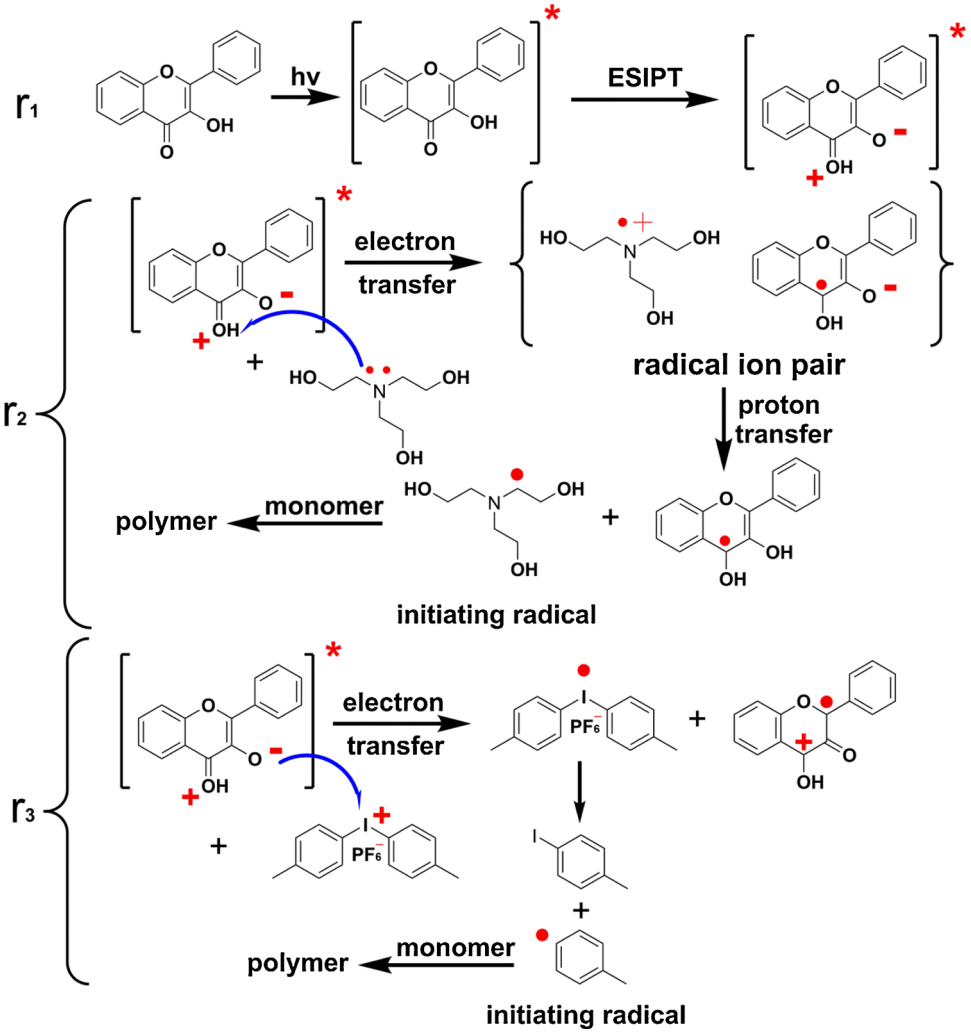


**Fig. 11.** Proposed mechanisms of polymerization initiation by **3HFs/TEOA** and **3HFs/ONI.**

### *3.4. Photopolymerization using **3HFs/TEOA** and **3HFs/ONI** as initiation system*

As amine co-initiators are important to **3HFs**, the effect of different amines including **TEOA**, **MP**, **TEA** and **NPG** on free radical polymerization was studied in our study. The photopolymerization profiles of **TPGDA** in the presence of **3HF-H/TEOA**, **3HF-H /MP**, **3HF-H/TEA** and **3HF-H/NPG** under the 385 nm **LED** light sources are shown in supporting information S26-S28. It has been found that the photopolymerization has the highest polymerization rate using **TEOA** as the co-initiator and it has the lowest polymerization rate using **NPG** as the co-initiator. So **TEOA** was chosen as an electron donor to discuss the effect of substituents on polymerization efficiency in this study.

Upon irradiation with the 385 nm **LED**, the double bond conversion rates versus the time curves of the photocurable resin films containing different **3HFs** were obtained, and the results are shown in Figs. 9 and 10.

As seen from Fig. 9a, the **3HFs/TEOA** (1.0%/3.0% w/w) two-component system could effectively initiate the **FRP** of **TPGDA**, and the double bond conversions for **3HF-H**, **3HF-B-F**, **3HF-B-Cl**, and **3HF-B-Br** were similar, approximately 83%. The order of polymerization rate was **3HF-B-Cl** > **3HF-B-Br** > **3HF-B-F** > **3HF-H** > **3HF-B-$CH_3$**. Fig. 9b shows that the conversion and polymerization rate of **3HF-B-F** and **3HF-B-Br** are higher than those of the corresponding **3HF-A-F** and **3HF-A-Br**. When the $R_2$ group was substituted, the electron-donating group caused a decrease in the polymerization rate, but the electron-withdrawing group accelerated the polymerization. When $R_1$ and $R_2$ were substituted by the same atom, the polymerization rate was lower at the $R_1$ position. In the **3HFs/TEOA** system, **3HFs** was photoreduced by **TEOA**. When the substituents make more electrons in **3HFs**, they are more difficult to be reduced by **TEOA**. Therefore, the electron donating groups reduce the initiation efficiency of the **3HFs/TEOA** initiation system.

In the **3HFs/ONI** initiation system, **3HFs** can be used as both a co-initiator and a primary initiator. As a co-initiator, the polymerization curve of **3HFs/ONI** (0.20%/1.0% w/w) is shown in Fig. 10a and b. Their conversions and rates are similar. When the B ring had substituents, the order of **FRP** rate was **3HF-B-$CH_3$** > **3HF-B-Cl** > **3HF-B-Br** > **3HF-B-F** > **3HF-H**. When $R_1$ and $R_2$ were substituted by the same atom, the order of **FRP** rate was **3HF-A-Br** > **3HF-A-F** > **3HF-B-Br** > **3HF-B-F** > **3HF-H**. When **3HFs** was used as the main initiator, the polymerization curve of **3HFs/ONI** (1.0%/0.20% w/w) was obtained, as shown in Fig. 10c and d. The conversion exceeded 80%. When the B ring had substituents, the order of **FRP** rate was **3HF-B-$CH_3$** > **3HF-B-F** > **3HF-B-Cl** > **3HF-B-Br** > **3HF-H.** When $R_1$ and $R_2$ were substituted by the same atom, the order of **FRP** rate was **3HF-A-Br** > **3HF-A-F** > **3HF-B-F** > **3HF-B- Br** > **3HF-H**. When $R_1$ and $R_2$ were replaced, the polymerization rate was accelerated. When $R_2$ was substituted, the electron-donating group had the greatest influence on the polymerization rate. When $R_1$ and $R_2$ were substituted by the same atom, they had a greater influence on the initiation efficiencies at the $R_1$ position.

In the **3HFs/ONI** system, **3HFs** were photo-oxidized by **ONI**. When

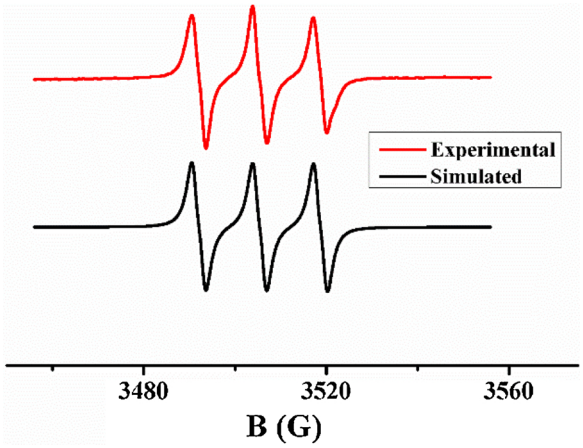


**Fig. 12.** ESR-ST spectra of radical generated in 3HF-H/ONI and trapped by PBN in tert-butylbenzene ([ONI] = 0.01 M) [25].

**Table 2**
Parameters characterizing the photochemical reactivity of the **3HFs** with **ONI** or **TEOA**: oxidation and reduction potentials ($E_{ox}$ and $E_{red}$); the excited state energy ($E_S$); free energy changes for the **3HFs/ONI** interaction ($\Delta G_S$**(ONI)**); free energy changes for the **3HFs/TEOA** interaction ($\Delta G_S$**(TEOA)**); $E_{red}$(ONI) = 0.06 V, $E_{ox}$ (TEOA) = 0.87 V in the methanol.

| 3-HF | $E_{ox}$ (V/SCE) | $E_{red}$ (V/SCE) | $E_S$ (eV) | $\Delta G_S$(eV) (ONI) | $\Delta G_S$(eV) (TEOA) |
|---|---|---|---|---|---|
| **3HF-H** | 1.05 | −0.92 | 3.27 | −2.28 | −1.48 |
| **3HF-B-CH$_3$** | 0.99 | −0.91 | 2.85 | −1.92 | −1.07 |
| **3HF-B-F** | 1.01 | −0.95 | 3.26 | −2.31 | −1.44 |
| **3HF-B-Cl** | 1.02 | −0.90 | 3.25 | −2.29 | −1.48 |
| **3HF-B-Br** | 1.01 | −0.89 | 3.24 | −2.29 | −1.48 |
| **3HF-A-F** | 1.03 | −0.88 | 3.13 | −2.16 | −1.38 |
| **3HF-A-Br** | 1.01 | −0.81 | 2.77 | −1.82 | −1.09 |

$E_{ox}$ and $E_{red}$ values vs. SCE ($E_{(Fc/Fc)}^{+}$ = 0.38 V vs. SCE [35], $E_{(Fc/Fc)}^{+}$ = 0.29 V vs. Ag/AgCl). Singlet state energies $E_S$ extracted from the UV–vis absorption and fluorescence emission spectra of the **3HFs** in the methanol. Free energy changes ($\Delta G_S$) were calculated from the classical Rehm–Weller equation.

the substituents increase electron density in **3HFs**, **3HFs** are more likely to be oxidized by **ONI**. Therefore, the electron donating groups accelerate the polymerization of the **3HFs/ONI** initiation system. The electron withdrawing group also accelerates the polymerization compared to unsubstituted because the **ONI** has higher reactivity.

### 3.5. Free radical polymerization mechanism

On the basis of the above study, we found that the laws of photopolymerization were inconsistent with those of the photolysis rate. Hence, the first photopolymerization process was excitation of **3HFs**, and then the charge transfer between **3HFs** and **TEOA** or **ONI** generated free radicals, which were the active species that initiated photopolymerization. The charge transfer between **3HFs** excited state and **TEOA** or **ONI** was the rate determining step of photopolymerization.

The proposed mechanism is shown in Fig. 11. In the **3HFs/TEOA** system, **3HFs** was photoreduced by **TEOA**. In the **3HFs/ONI** system, **3HFs** was photo-oxidized by **ONI**. Oxidation and reduction are two opposite processes. Hence, substituents should have different effects on the photoinitiation efficiencies. Although halogen also accelerated the rate of polymerization in the **3HFs/ONI** system, it might be due to the high oxidative activity of the iodonium salt.

In the **3HFs/TEOA** initiating system, the **3HFs** underwent excitation, then a proton transfer to form a tautomer **(r1)**, and finally a charge transfer with the amine to form a radical cation **(TEOA$^{\cdot+}$)** and a radical anion **(3HF$^{\cdot-}$)**. The radical ion pair then underwent proton transfer to produce the the corresponding aminoalkyl radical, capable for initiation of polymerization, and a less reactive 3HF-derived radical, which probably underwent other radical reactions (r2). In the case of **3HFs/ONI** initiating system, proton transfer occurred to generate tautomers **(r1)**. Then, the tautomer and the **ONI** underwent charge transfer to generate a radical cation **(3HF$^{\cdot+}$)** and an unstable onium salt radical. Unstable onium salt radical produced tolyl radical-initiated polymerization. The radical cation **(3HF$^{\cdot+}$)** probably underwent deprotonation and other chemical reactions.

**ESR-ST** spectra of tert-butylbenzene solution of **3HF/ONI/PBN** were obtained upon irradiation (**385 nm LED**). Following electron transfer in the **3HFs** and **ONI** under light irradiation, radical cations (e.g. **3HF$^{\cdot+}$**) and toluene radicals Ph. were detected in ESR experiments (Fig. 12) [25].

### 3.6. Free energy changes of photoinduced electron transfer

The $E_{ox}$ **(V/SCE)** and $E_{red}$ **(V/SCE)** values of the **3HFs** were measured by cyclic voltammetry by using a CHI760E electrochemical workstation. As seen from Table 2, the $\Delta G_S$ **(TEOA)** and $\Delta G_S$ **(ONI)** values are all negative, which prove that the charge transfer between **3HFs** and **TEOA/ONI** is thermodynamically favorable.

## 4. Conclusions

**3HFs** with different substituents show a wide absorption from 280 to 450 nm and different absorption strengths caused by the substituents. The substituents also affect the emission at approximately 400 nm caused by the **ESIPT** process. The steady-state photolysis and fluorescence quenching of **3HFs** under the 385 nm **LED** light source showed that the proton transfer reaction preceded the charge transfer reaction between **3HFs** and triethanolamine **(TEOA)** or iodonium salts **(ONI)**, and groups with different electron properties could affect the photochemistry of **3HFs.** The **3HFs/TEOA** and **3HFs/ONI** two-component systems can effectively initiate the **FRP** of **TPGDA**. Substituents affect the initiation efficiency differently in the **3HFs/TEOA** and **3HFs/ONI** system.

## Declaration of Competing Interest

The authors declare no competing financial interest.

## Acknowledgements

The authors thank the National Key Research and Development Program of China (2017YFB0307800) and Science and Technology Planning Project of Guangdong Province, China (project No. 2017B090911002) for financial support. We also thank the Beijing University of Chemical Technology CHEMCLOUDCOMPUTING Platform for support with calculations. The authors also thank the State Key Laboratory of Optoelectronic Materials and Technologies (Sun Yat-sen University) (project no. OEMT-2018-KF-12).

## Appendix A. Supplementary data

Supplementary material related to this article can be found, in the online version, at doi:https://doi.org/10.1016/j.jphotochem.2019.112097.

## References

[1] Y.J. Rao, T. Sowjanya, G. Thirupathi, N.Y.S. Murthy, S.S. Kotapalli, Synthesis and biological evaluation of novel flavone/triazole/benzimidazole hybrids and flavone/isoxazole-annulated heterocycles as antiproliferative and antimycobacterial agents, Mol. Divers. 22 (4) (2018) 803–814, https://doi.org/10.1007/s11030-018-9833-4.
[2] H. Yoo, S.-H. Kim, J.-Y. Lee, H.-J. Kim, S.-H. Seo, B.-Y. Chung, C.-B. Jin, Y.-S. Lee, Synthesis and antioxidant activity of 3-methoxyflavones, Korean, Chem. Soc. 26

(2005) 2057–2060, https://doi.org/10.5012/bkcs.2005.26.12.2057.
[3] N. Balasuriya, H.P.V. Rupasinghe, Antihypertensive properties of flavonoid-rich apple peel extract, Food Chem. 135 (2012) 2320–2325, https://doi.org/10.1016/j.foodchem.2012.07.023.
[4] J. Li, B. Xue, Q. Chai, Z. Liu, A. Zhao, L.J. Chen, Antihypertensive effect of total flavonoid fraction of Astragalus complanatus in hypertensive rats, Chin. J. Physiol. 48 (2) (2005) 101.
[5] M. Kawai, T. Hirano, S. Higa, J. Arimitsu, M. Maruta, Y. Kuwahara, T. Ohkawara, K. Hagihara, T. Yamadori, Y. Shima, Flavonoids and related compounds as anti-allergic substances, Allergol. Int. 56 (2007) 113–123, https://doi.org/10.2332/allergolint.R-06-135.
[6] D.D. Orhan, B. Özçelik, S. Özgen, F. Ergun, Antibacterial, antifungal, and antiviral activities of some flavonoids, Microbiol. Res. 165 (2010) 496–504, https://doi.org/10.1016/j.micres.2009.09.002.
[7] T. Inoue, Y. Sugimoto, H. Masuda, C.J. Kamei, Antiallergic effect of flavonoid glycosides obtained from Mentha piperita L, Biol. Pharm. Bull. 25 (2002) 256–259, https://doi.org/10.1248/bpb.25.256.
[8] R.J. Nijveldt, E. Van Nood, D.E. Van Hoorn, P.G. Boelens, K. Van Norren, P.A. Van Leeuwen, Flavonoids: a review of probable mechanisms of action and potential applications, Am. J. Clin. Nutr. 74 (2001) 418–425, https://doi.org/10.1093/ajcn/74.4.418.
[9] A.M. Forbes, H. Lin, G.G. Meadows, G.P. Meier, Synthesis and anticancer activity of new flavonoid analogs and inconsistencies in assays related to proliferation and viability measurements, Int. J. Oncol. 45 (2014) 831–842, https://doi.org/10.3892/ijo.2014.2452.
[10] P.K. Sengupta, M. Kasha, Excited state proton-transfer spectroscopy of 3-hydroxyflavone and quercetin, Chem. Phys. Lett. 68 (1979) 382–385, https://doi.org/10.1016/0009-2614(79)87221-8.
[11] A.J.G. Strandjord, S. Courtney, D. Friedrich, P. Barbara, Excited-state dynamics of 3-hydroxyflavone, J. Phys. Chem. 87 (1983) 1125–1133.
[12] D. McMorrow, M. Kasha, Intramolecular excited-state proton transfer in 3-hydroxyflavone. Hydrogen-bonding solvent perturbations, J. Phys. Chem. 88 (1984) 2235–2243.
[13] B.J. Schwartz, L.A. Peteanu, C.B. Harris, Direct observation of fast proton transfer: femtosecond photophysics of 3-hydroxyflavone, J. Phys. Chem. 96 (1992) 3591–3598.
[14] S. Ameer-Beg, S.M. Ormson, R.G. Brown, P. Matousek, M. Towrie, E.T. Nibbering, P. Foggi, F. Neuwahl, Ultrafast measurements of excited state intramolecular proton transfer (ESIPT) in room temperature solutions of 3-hydroxyflavone and derivatives, J. Phys. Chem.-A. 105 (2001) 3709–3718, https://doi.org/10.1021/jp0031101.
[15] A.D. Roshal, A.V. Grigorovich, A.O. Doroshenko, V.G. Pivovarenko, A.P. Demchenko, Flavonols as metal-ion chelators: complex formation with $Mg^{2+}$ and $Ba^{2+}$ cations in the excited state, J. Photochem. Photobiol. A: Chem. 127 (1–3) (1999) 89–100, https://doi.org/10.1016/S1010-6030(99)00105-7.
[16] G.J. Smith, K.R. Markham, Tautomerism of flavonol glucosides: relevance to plant UV protection and flower colour, J. Photochem. Photobiol. A: Chem. 118 (2) (1998) 99–105, https://doi.org/10.1016/S1010-6030(98)00354-2.
[17] W. Feng, Y. Wang, S. Chen, C. Wang, S. Wang, S. Li, H. Li, G. Zhou, J. Zhang, 4-Nitroimidazole-3-hydroxyflavone conjugate as a fluorescent probe for hypoxic cells, Dye. Pigment. 131 (2016) 145–153, https://doi.org/10.1016/j.dyepig.2016.03.019.
[18] C. Dyrager, A. Friberg, K. Dahlen, M. Fridén-Saxin, K. Börjesson, L.M. Wilhelmsson, M. Smedh, M. Grøtli, K. Luthman, 2, 6, 8-trisubstituted 3-hydroxychromone derivatives as fluorophores for live-cell imaging, Chem. Eur. J. 15 (2009) 9417–9423, https://doi.org/10.1002/chem.200900279.
[19] S. Chen, P. Hou, B. Zhou, X. Song, J. Wu, H. Zhang, J. Foley, A red fluorescent probe for thiols based on 3-hydroxyflavone and its application in living cell imaging, RSC Adv. 3 (2013) 11543–11546, https://doi.org/10.1039/C3RA41554F.
[20] B. Liu, Z.J. Luo, S.F. Si, X.F. Zhou, C.J. Pan, L. Wang, A photostable triphenylamine-based flavonoid dye: Solvatochromism, aggregation-induced emission enhancement, fabrication of organic nanodots, and cell imaging applications, Dye. Pigment. 142 (2017) 32–38, https://doi.org/10.1016/j.dyepig.2017.03.023.
[21] L.Y. Dong, L.Y. Wang, X.F. Wang, Y. Liu, H.L. Liu, M.X. Xie, Development of fluorescent FRET probe for determination of glucose based on β-cyclodextrin modified ZnS-quantum dots and natural pigment 3-hydroxyflavone, Dye. Pigment. 128 (2016) 170–178, https://doi.org/10.1016/j.dyepig.2016.01.032.
[22] V.I. Tomin, D.V. Ushakou, Use of 3-hydroxyflavone as a fluorescence probe for the controlled photopolymerization of the E-shell 300 polymer, Polym. Test. 64 (2017) 77–82, https://doi.org/10.1016/j.polymertesting.2017.09.036.
[23] J.C. Zhao, J. Lalevée, H.X. Lu, R. MacQueen, S.H. Kable, T.W. Schmidt, M.H. Stenzel, P. Xiao, A new role of curcumin: as a multicolor photoinitiator for polymer fabrication under household UV to red LED bulbs, Polym. Chem. 6 (2015) 5053–5061, https://doi.org/10.1039/C5PY00661A.
[24] W.X. Han, H.Y. Fu, T.L. Xue, T.Z. Liu, Y. Wang, T. Wang, Facilely prepared blue-green light sensitive curcuminoids with excellent bleaching properties as high performance photosensitizers in cationic and free radical photopolymerization, Polym. Chem. 9 (2018) 1787–1798, https://doi.org/10.1039/C8PY00166A.
[25] M.-A. Tehfe, F. Dumur, P. Xiao, B. Graff, F. Morlet-Savary, J.-P. Fouassier, D. Gigmes, J. Lalevée, New chromone based photoinitiators for polymerization reactions under visible light, Polym. Chem. 4 (2013) 4234–4244, https://doi.org/10.1039/C3PY00536D.
[26] A. Al Mousawi, P. Garra, M. Schmitt, J. Toufaily, T. Hamieh, B. Graff, J.P. Fouassier, F. Dumur, J. Lalevée, 3-Hydroxyflavone and N-phenylglycine in high performance photoinitiating systems for 3D printing and photocomposites synthesis, Macromolecules 51 (2018) 4633–4641, https://doi.org/10.1021/acs.macromol.8b00979.
[27] J. Algar, J.P. Flynn, A New Method for the Synthesis of Flavonols, (1934).
[28] R. Khanna, R. Kumar, A. Dalal, R.C.J. Kamboj, Absorption and fluorescent studies of 3-Hydroxychromones, J. Fluoresc. 25 (2015) 1159–1163, https://doi.org/10.1007/s10895-015-1623-0.
[29] V.S. Dofe, A.P. Sarkate, D.K. Lokwani, S.H. Kathwate, C.H. Gill, Synthesis, antimicrobial evaluation, and molecular docking studies of novel chromone based 1, 2, 3-triazoles, Res. Chem. Intermediat. 43 (2017) 15–28, https://doi.org/10.1007/s11164-016-2602-z.
[30] A. Kurzwernhart, W. Kandioller, S. Bächler, C. Bartel, S. Martic, M. Buczkowska, G. Mühlgassner, M.A. Jakupec, H.-B. Kraatz, P.J. Bednarski, Structure–activity relationships of targeted RuII (η6-p-cymene) anticancer complexes with flavonol-derived ligands, J. Med. Chem. 55 (2012) 10512–10522, https://doi.org/10.1021/jm301376a.
[31] A. Hasan, L. Rasheed, A. Malik, Synthesis and characterization of variably halogenated chalcones and flavonols and their antifungal activity, Asian. J. Chem. 19 (2007) 937.
[32] J.W. Stansbury, S.H. Dickens, Determination of double bond conversion in dental resins by near infrared spectroscopy, Dent. Mater. 17 (2001) 71–79, https://doi.org/10.1016/S0109-5641(00)00062-2.
[33] R.R. Gagne, C.A. Koval, G.C. Lisensky, Ferrocene as an internal standard for electrochemical measurements, Inorg. Chem. 19 (1980) 2854–2855.
[34] V.V. Pavlishchuk, A.W. Addison, Conversion constants for redox potentials measured versus different reference electrodes in acetonitrile solutions at 25 C, Inorg. Chim. Acta 298 (2000) 97–102, https://doi.org/10.1016/S0020-1693(99)00407-7.
[35] D. Rehm, A. Weller, Kinetics of fluorescence quenching by electron and H-atom transfer, Isr. J. Chem. 8 (1970) 259–271, https://doi.org/10.1002/ijch.197000029.
[36] D. Goltz, S. Ahmadi, J. Crawford, D. Craig, Photochemical properties of selected flavonol dyes: effects on their separation using capillary electrophoresis, J. Liq. Chromatogr. R. T. 39 (2016) 768–774, https://doi.org/10.1080/10826076.2016.1247714.
[37] A. Villela, M.S.A. van Vuuren, H.M. Willemen, G.C.H. Derksenb, T.A. van Beeka, Photo-stability of a flavonoid dye in presence of aluminium ions, Dye. Pigment. 162 (2019) 222–231, https://doi.org/10.1016/j.dyepig.2018.10.021.
[38] C. Mouri, V. Mozaffarian, X. Zhang, R. Laursen, Characterization of flavonols in plants used for textile dyeing and the significance of flavonol conjugates, Dye. Pigment. 100 (2014) 135–141, https://doi.org/10.1016/j.dyepig.2013.08.025.
[39] H. Chaaban, I. Ioannou, C. Paris, C. Charbonnela, M. Ghoul, The photostability of flavanones, flavonols and flavones and evolution of their antioxidant activity, J. Photochem. Photobiol. A: Chem. 336 (2017) 131–139, https://doi.org/10.1016/j.jphotochem.2016.12.027.
[40] G.J. Smith, S.J. Thomsen, K.R. Markham, C. Andary, D. Cardon, The photostabilities of naturally occurring 5-hydroxyflavones, flavonols, their glycosides and their aluminium complexes, J. Photochem. Photobiol. A: Chem. 136 (1–2) (2000) 87–91, https://doi.org/10.1016/S1010-6030(00)00320-8.
[41] G.J. Woolfe, P.J. Thistlethwaite, Direct observation of excited state intramolecular proton transfer kinetics in 3-hydroxyflavone, J. Am. Chem. Soc. 103 (1981) 6916–6923.
[42] M. Itoh, K. Tokumura, Y. Tanimoto, Y. Okada, H. Takeuchi, K. Obi, I. Tanaka, Time-resolved and steady-state fluorescence studies of the excited-state proton transfer in 3-hydroxyflavone and 3-hydroxychromone, J. Am. Chem. Soc. 104 (1982) 4146–4150.
[43] M. Itoh, Y. Fujiwara, Two-step laser excitation fluorescence study of the ground-and excited-state proton transfer in 3-hydroxyflavone and 3-hydroxychromone, J. Phys. Chem. 87 (1983) 4558–4560.
[44] N.P. Ernsting, B. Dick, Fluorescence excitation of isolated, jet-cooled 3-hydroxyflavone: the rate of excited state intramolecular proton transfer from homogeneous linewidths, Chem. Phys. 136 (1989) 181–186, https://doi.org/10.1016/0301-0104(89)80045-X.
[45] M. Sarkar, P.K. Sengupta, Influence of different micellar environments on the excited-state proton-transfer luminescence of 3-hydroxyflavone, Chem. Phys. Lett. 179 (1991) 68–72, https://doi.org/10.1016/0009-2614(91)90293-I.
[46] B. Dick, AM1 and INDO/S calculations on electronic singlet and triplet states involved in excited-state intramolecular proton transfer of 3-hydroxyflavone, J. Phys. Chem. 94 (1990) 5752–5756.
[47] M.L. Martinez, S.L. Studer, P.T. Chou, Direct evidence of the triplet-state origin of the slow reverse proton transfer reaction of 3-hydroxyflavone, J. Am. Chem. Soc. 112 (1990) 2427–2429.
[48] I. Yokoe, K. Higuchi, Y. Shirataki, M. Komatsu, Photochemistry of flavonoids. III. Photorearrangement of flavonols, Chem. Pharm. Bull. 29 (1981) 894–898, https://doi.org/10.1248/cpb.29.894.
[49] T. Matsuura, T. Takemoto, R. Nakashima, Photoinduced reactions—LXXI: photorearrangement of 3-hydroxyflavones to 3-aryl-3-hydroxy-1, 2-indandiones, Tetrahedron 29 (1973) 3337–3340, https://doi.org/10.1016/S0040-4020(01)93485-4.
[50] Š. Ramešová, R. Sokolová, I. Degano, The study of the oxidation of the natural flavonol fisetin confirmed quercetin oxidation mechanism, Electrochim. Acta 182 (2015) 544–549, https://doi.org/10.1016/j.electacta.2015.09.144.
[51] P.-G. Pietta, Flavonoids as antioxidants, J. Nat. Prod. 63 (2000) 1035–1042, https://doi.org/10.1021/np9904509.
[52] G. Agati, E. Azzarello, S. Pollastri, M. Tattini, Flavonoids as antioxidants in plants: location and functional significance, Plant Sci. 196 (2012) 67–76, https://doi.org/10.1016/j.plantsci.2012.07.014.